The Journal of Chemical Physics ARTICLE scitation.org/journal/jcp

Transmembrane potential of physiologically relevant model membranes: Effects of membrane asymmetry

Cite as: J. Chem. Phys. 153, 105103 (2020); doi: 10.1063/5.0018303
Submitted: 13 June 2020 • Accepted: 18 August 2020 •
Published Online: 8 September 2020

Xubo Lin[1,a] and Alemayehu A. Gorfe[2,a]

AFFILIATIONS

[1] Institute of Single Cell Engineering, Beijing Advanced Innovation Center for Biomedical Engineering, Beihang University, Beijing 100191, China

[2] Department of Integrative Biology and Pharmacology, McGovern Medical School, The University of Texas Health Science Center at Houston, Houston, Texas 77030, USA

Note: This paper is part of the JCP Special Topic on Classical Molecular Dynamics (MD) Simulations: Codes, Algorithms, Force Fields, and Applications.

[a] **Authors to whom correspondence should be addressed:** linxbseu@buaa.edu.cn and alemayehu.g.abebe@uth.tmc.edu

ABSTRACT

Transmembrane potential difference (V_m) plays important roles in regulating various biological processes. At the macro level, V_m can be experimentally measured or calculated using the Nernst or Goldman–Hodgkin–Katz equation. However, the atomic details responsible for its generation and impact on protein and lipid dynamics still need to be further elucidated. In this work, we performed a series of all-atom molecular dynamics (MD) simulations of symmetric model membranes of various lipid compositions and cation contents to evaluate the relationship between membrane asymmetry and V_m. Specifically, we studied the impact of the asymmetric distribution of POPS (1-palmitoyl-2-oleoyl-sn-*glycero*-3-phospho-L-serine), PIP2 (phosphatidylinositol 4,5-bisphosphate), as well as Na^+ and K^+ on V_m using atomically detailed MD simulations of symmetric model membranes. The results suggest that, for an asymmetric POPC-POPC/POPS bilayer in the presence of NaCl, the presence of the monovalent anionic lipid POPS in the inner leaflet polarizes the membrane ($\Delta V_m < 0$). Intriguingly, replacing a third of the POPS lipids by the polyvalent anionic signaling lipid PIP2 counteracts this effect, resulting in a smaller negative membrane potential. We also found that replacing Na^+ ions in the inner region by K^+ depolarizes the membrane ($\Delta V_m > 0$). These divergent effects arise from variations in the strength of cation–lipid interactions and are correlated with changes in lipid chain order and head-group orientation.

INTRODUCTION

The physiologic transmembrane potential (V_m) represents the difference in electrical potential between the extracellular and intracellular compartments of the cell. The magnitude of the V_m in resting cells varies from cell to cell but generally ranges from about −10 mV to −100 mV.[1] It is well known that fluctuations in electrical signals play many essential roles in the cell. For instance, in nerve cells, changes in V_m regulate the amplitude and duration of somatic and axonal action potentials.[2] Changes in V_m can also alter the membrane permeability of many ions and other small molecules[3] that are critical for cell fate decisions and maintenance of the homeostatic balance.[4,5] Therefore, cells employ sophisticated mechanisms, such as the regulated opening and closing of ion channels, to control the extent of plasma membrane depolarization (reduction in V_m) or hyperpolarization (larger negative V_m). A phenomenon less well-understood at the molecular level is how changes in V_m might alter the organization of plasma membrane lipids and proteins to modulate signaling events underlying cell growth and proliferation. This fundamental biophysical problem has important implications to pathophysiology including cancer. For example, it has been shown that depolarization enhances the nanoscale clustering and activation

of the oncogenic protein K-Ras, resulting in enhanced signaling and cell proliferation.[6] This was proposed to arise from changes in the lateral dynamics of 1-palmitoyl-2-oleoyl-sn-*glycero*-3-phospho-L-serine (POPS) and phosphatidylinositol 4,5-bisphosphate (PIP2) lipids.[6] Therefore, it is important to understand not only the atomic basis of V_m but also how it might depend on and, in turn, affect the structure and dynamics of membrane components. The focus of the current work is to examine the effect of membrane compositional asymmetry and ion distribution on V_m.

Although its exact lipid composition may depend on the cell status and varies from cell type to cell type, a large body of previous research has established a general picture of the plasma membrane lipid composition and ion distribution:[7,8] (1) Some of the most common phospholipids such as 1-palmitoyl-2-oleoyl-sn-*glycero*-3-phosphocholine (POPC) are found on both sides of the plasma membrane. (2) The intracellular leaflet is enriched in anionic lipids such as POPS and phosphatidylinositol. (3) There are more sodium ions in the extracellular space and more potassium ions in the cytosol. In this work, we systematically studied the impact of the asymmetric distribution of POPC, POPS, PIP2, as well as Na^+ and K^+ on V_m using atomically detailed molecular dynamics (MD) simulations. The results suggest that, for an asymmetric PC-PC/PS bilayer in the presence of NaCl salt, the presence of POPS in the inner leaflet polarizes the membrane ($\Delta V_m < 0$). Interestingly, replacing a third of the PS lipids by PIP2 largely counteracts this effect, resulting in a smaller negative membrane potential. Intracellular K^+ depolarizes the membrane ($\Delta V_m > 0$). These effects arise from differences in the strength of cation–lipid interactions and are correlated with changes in lipid chain order and head-group orientation.

METHODS

MD simulation is a powerful tool to probe the atomic details associated with transmembrane potential generation and impact.[9,10] Previous MD simulations used coarse-grained,[11] united-atom,[12] all-atom,[13] and polarizable[14] models to estimate the V_m of a variety of lipid bilayers. These models yielded dramatically different electrostatic potential profiles. This is especially true in the hydrocarbon chain region, where the shape of the plot of the potential vs an axis along the membrane normal is flatter in coarse-grained and united-atom models than in all-atom and polarizable models. This can be ascribed to the different treatment of partial charges to atoms or interaction sites in these models. Nonetheless, V_m values obtained from all models range from a few tens of millivolts to around one hundred millivolts, which is roughly comparable to the experimental data.[1] Here, we chose to use an all-atom model[15] in order to capture the motion of every atom in a comparatively cost-effective manner (relative to polarizable force fields).

Calculating V_m of an asymmetric membrane from simulations of two symmetric membranes

An accurate calculation of V_m from MD simulation depends on how well the charge distribution is sampled along the membrane normal. However, it is not always easy to achieve convergence of the charge distribution. Let us consider, for example, a two-bilayer all-atom simulation system with no charge imbalance between leaflets

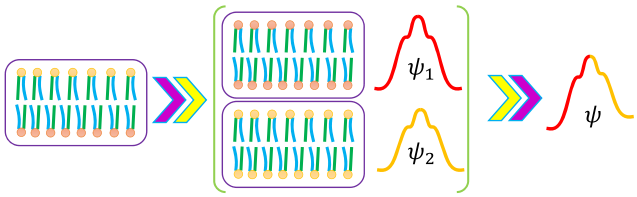

SCHEME 1. Estimating the electrostatic potential (ψ) of an asymmetric membrane using two symmetric membranes. ψ_1 and ψ_2 are the symmetric electrostatic potential profiles obtained from the symmetrized charge distribution profiles of the respective symmetric membranes.

($\Delta Q = 0$). If this system is made up of single-component symmetric lipids, it is relatively easy to achieve convergence within a simulation time of hundreds of nanoseconds. This would yield a high-quality electrostatic potential profileScheme [9,12] that is mirror-symmetric with respect to the mid-plane of the bilayer, and the final V_m would be zero, as expected. However, if the bilayer is composed of multiple lipid types, which is more physiological, even a μs-scale simulation is not sufficient to obtain a mirror-symmetric electrostatic potential profile. For example, our previous all-atom MD simulation study found an unacceptably high $V_m \approx 40$ mV with $\Delta Q = 0$ (expected: $V_m \approx 0$ mV).[13] In multi-component, asymmetric bilayers, the problem is compounded by several factors. (i) Lipid compositional asymmetry can result in local bilayer deformation. Although this is less of a problem for our small membrane systems, uneven lateral pressures and kinetically trapped non-equilibrium states may still happen, which could complicate the accurate calculation of charge density along the membrane normal within a limited simulation time. (ii) Ions can passively equilibrate across the membrane, making it difficult to maintain an exactly identical ion distribution, which is necessary to obtain a symmetric charge density profile for a symmetric membrane system. To avoid these complications and obtain a reliable estimate of V_m for multi-component asymmetric membranes, two separate simulations can be conducted: one representing the outer leaflet of the plasma membrane and another representing the inner leaflet. Then, in each case, the charge density distribution $\rho(z)$ ($z = 0$ being the bilayer center) is averaged over the two halves (effectively symmetrized with respect to the membrane center of mass) as $\rho(z) = (\rho(-z) + \rho(+z))/2$. Thus, for the individual symmetric systems, the symmetrized $\rho(z)$ results in symmetric $\psi(z)$ and thus eliminates a non-zero V_m. To model the V_m of asymmetric membranes, we combined the symmetric $\psi(z)$ profiles of two symmetric membrane systems (Scheme 1) such that one represents the extracellular region ($z < 0$) and the other stands for the intracellular region ($z \geqslant 0$); the recombinant $\psi(z)$ then yields an effective transmembrane potential for the asymmetric membrane.[16] We used this approach to estimate the electrostatic potential of four asymmetric membrane systems based on the bilayers listed in Table I.

MD simulation

The CHARMM36 force field[15] was used to perform all-atom MD simulations on five symmetric single-bilayer systems (Table I). The initial configuration for each system was prepared using

TABLE I. Symmetric membrane systems simulated in this work.

System name	No. of lipids			No. of ions		
	POPC	POPS	PIP2[a]	Na^+	K^+	Cl^-
PC	200	0	0	32	0	32
PC/PS	140	60	0	92	0	32
PC/PS/K	140	60	0	0	92	32
PC/PS/PIP2	140	40	20	172	0	32
PC/PS/PIP2/K	140	40	20	0	172	32

[a]Data for the protonated PIP2 are provided in the supplementary material. Each simulation was run for 350 ns, and the first 50 ns was considered equilibrium phase, while the last 300 ns data were used for analysis by dividing into six 50 ns blocks. Each system was charge-neutralized (some of the Na^+ or K^+ ions were used as charge-neutralizing counterions), and the Cl^- concentration is 150 mM.

CHARMM-GUI.[17,18] The simulations were run under the constant pressure and temperature (NPT) ensemble with lipids, water, and ions separately coupled to a Nose–Hoover heat bath[19,20] at T = 310 K (coupling constant τ = 1 ps) and a pressure of 1 bar maintained by a semi-isotropic Parrinello–Rahman pressure coupling scheme[21] (coupling constant τ = 5 ps and compressibility = 4.5×10^{-5} $bars^{-1}$). The leap-frog Verlet algorithm and a periodic boundary condition [with bonds involving hydrogen atoms constrained using the LINear Constraint Solver (LINCS) algorithm[22]] were used. The Lennard-Jones potential was smoothly shifted to zero between 1.0 nm and 1.2 nm, and particle mesh Ewald (PME) electrostatics[23] was used with a real space cutoff of 1.2 nm. The non-bonded interaction neighbor list was updated every 20 steps with a cutoff of 1.2 nm. Simulations were run using GROMACS (version 2016.04)[24] for 350 ns with a time step of 2 fs, and coordinates were saved every 4 ps for analysis. Snapshots were rendered using Visual Molecular Dynamics (VMD).[25]

TRAJECTORY ANALYSIS

Mass/charge density calculation

Electrostatic potential $\psi(z)$ is calculated as the double integral of the charge density $\rho(z)$ along the membrane normal (z) using the Poisson equation,[9]

$$\psi(z) = -\int_{-z}^{z} dz' \int_{-z'}^{z'} \frac{1}{\varepsilon_0 \varepsilon_r} \rho(z'') dz'', \quad (1)$$

where ε_0 is the dielectric constant of vacuum (8.854×10^{-12} F m^{-1}) and $\varepsilon_r = 1$ in all-atom MD simulations. The accuracy of $\psi(z)$ depends on the calculation of $\rho(z)$. In our NPT simulations, the z-dimension of the simulation box fluctuates, and the z-location of the membrane center of mass may change over time. Hence, a direct application of the GROMACS tool *gmx density*, which bins the membrane along the z-dimension of the simulation box to calculate the mass and charge density profiles, may give rise to an inaccurate $\rho(z)$. Instead, we used an *in-house* script (based on "*xdrfile-1.1.4*," an open source program) that re-calculates the membrane center (z = 0 nm) and equally divides the range $|\Delta z| < 4$ nm to obtain the mass or charge distribution for each trajectory frame (a bin width of 0.05 nm was used in the current work). The final mass or charge density profile is obtained by averaging over all frames. As for error analysis, the last 300 ns of the 350 ns MD trajectories were divided into six equal blocks, and the standard deviation is obtained from block averaging.

Lipid acyl chain order parameter

As a direct measure of the structural flexibility of lipids, the lipid chain order parameter, S_{CH}, can be calculated as follows:

$$S_{CH} = \frac{1}{2}\langle 3\cos^2\theta - 1 \rangle, \quad (2)$$

where θ is the angle between the C–H vector and the membrane normal. S_{CH} is calculated using an *in-house* script based on the "*xdrfile-1.1.4*" program.

Lipid head tilt angle

For POPC and POPS lipids, the vector connecting the P atom and N atom was used to quantify lipid head orientation. For PIP2, the vector connecting the first and fourth carbon atoms in the six-membered carbon ring was used. The angle between these vectors and the membrane normal was defined as the lipid head tilt angle, which was also calculated using an *in-house* script based on the "*xdrfile-1.1.4*" program.

Lipid-ion contact probability

The contacts between atoms in lipids and ions were counted when the distance between them was less than 0.3 nm. The contact probability of ions separately with POPC, POPS, or PIP2 lipids was then obtained by dividing the number of contacts with each lipid type by the total number of contacts with all lipids and then averaged over all frames of the last 300 ns data. Visualization of the final snapshots was achieved by VMD[25] using the "beta" coloring method, where the "B-factor" columns in the *pdb* files of lipids were replaced by the calculated contact probability.

RESULTS AND DISCUSSION

V_m of asymmetric membranes from symmetric model membranes

Previous MD studies have shown that it is difficult to obtain a symmetric electrostatic potential profile for multi-component bilayers. For such systems, insufficient sampling[13] presents an additional challenge. Therefore, we followed a similar approach to that used by Falkovich *et al.*[16] and simulated symmetric membranes whose lipid composition roughly models the inner and outer leaflets of the plasma membrane to estimate the V_m of asymmetric model membranes (see the section titled Methods). We used a pure POPC bilayer as a simplified model of the plasma membrane outer leaflet. The inner leaflet is modeled by a two-component lipid bilayer POPC/POPS (0.7:0.3) or a three-component bilayer POPC/POPS/PIP2 (0.7:0.2:0.1), reflecting the enrichment of these anionic lipids in the inner leaflet of the plasma membrane. We realize that the inner leaflet also contains other neutral lipids such as

phosphatidylethanolamine (PE). However, for simplicity, here, we assume that the outer leaflet can be modeled by a pure POPC bilayer and the inner leaflet by a PC plus PS ± phosphatidylinositol (but not PE). The three systems were simulated in the presence of NaCl and

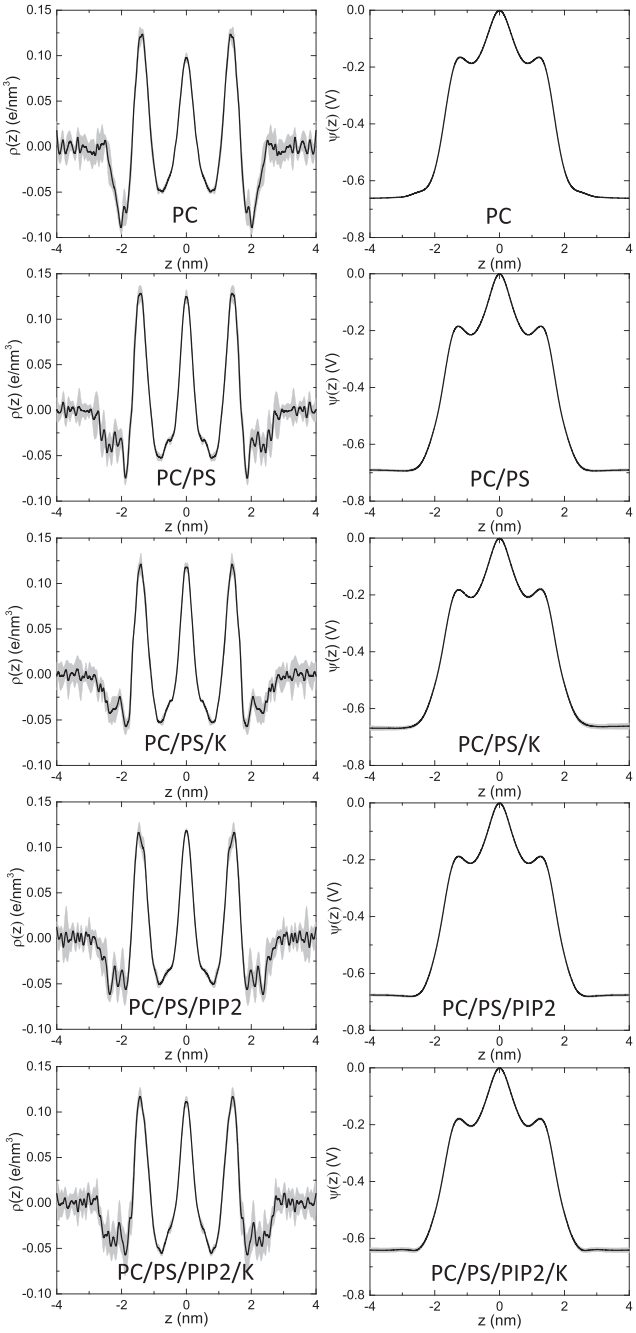

FIG. 1. Symmetrized charge density distribution (left column) and electrostatic potential (right column) profiles of the five symmetric systems simulated in this work. A bin width of 0.05 nm was used, and error bars (standard deviations) are shown in gray. The non-symmetrized charge density profiles are shown in Fig. S1.

are referred to as PC, PC/PS, and PC/PS/PIP2 (Table I), respectively. To examine the impact of potassium ions on the inner leaflet of the plasma membrane, we ran two additional simulations in which Na^+ was replaced by K^+ (systems PC/PS/K and PC/PS/PIP2/K).

Figure 1 (left) shows the charge density distribution along the membrane normal, $\rho(z)$, for each of the five systems simulated in this work. Note that for each frame of the last 300 ns of each trajectory, $\rho(z)$ was symmetrized over the two halves of the bilayer centered at z = 0. Using Eq. (1) and setting $\psi(0) = 0$ mV, we obtained the corresponding symmetric electrostatic potential [$\psi(z)$] profiles (Fig. 1, right). As illustrated in Scheme 1, each $\psi(z)$ profile derived from each model membrane representing the inner leaflet of the plasma membrane (systems PC/PS, PC/PS/K, PC/PS/PIP2, and PC/PS/PIP/K) was combined with that of the outer leaflet $\psi(z)$ (system PC) to obtain recombinant $\psi(z)$ profiles for the asymmetric PC-PC/PS, PC-PC/PS/K, PC-PC/PS/PIP2, and PC-PC/PS/PIP2/K membranes [Fig. 2(a)]. In these plots, -4 nm < z < 0 nm represents the outer leaflet of the membrane made up of pure PC lipids, while the region 0 nm ≤ z < 4 nm presents the inner leaflet and is modeled by PC/PS, PC/PS/K, PC/PS/PIP2, or PC/PS/PIP2/K. The transmembrane potential difference is then calculated as $V_m = \psi(4) - \psi(-4)$, and the results are shown in Fig. 2(b).

PS and PS/PIP2 in the inner membrane leaflet contribute differently to V_m

The electrostatic potential difference across the membranes (V_m) was calculated as the difference in $\psi(z)$ values in the bulk water regions of the inner and outer leaflets: $V_m = \psi(4) - \psi(-4)$. For all the symmetric bilayer systems (Fig. 1), $\psi(z)$ values at z = ± 4 are identical as expected ($V_m = 0$ mV). These symmetric $\psi(z)$ profiles were then recombined into the asymmetric $\psi(z)$ profiles for the four asymmetric membranes (Fig. 2). The results show that replacing 30% of the inner leaflet POPC lipids by POPS (net charge: $-1e$) resulted in the decrease in $\psi(\pm4)$ from −0.661 V to −0.690 V (Fig. 1) and thus an effective V_m of ∼−29 mV for the asymmetric PC-PC/PS system in the presence of Na^+ ions (Fig. 2). Note that the change in V_m from 0 mV to ∼−29 mV is not caused by charge imbalance because counterions were used for each of the PC and PC/PS simulations to keep the system neutral. In other words, POPS has a polarizing effect on the lipid membrane, which is consistent with the previous united-atom MD simulation results of a PC-PS system.[26] Intriguingly, replacing a third of the POPS lipids with the polyvalent anionic lipid PIP2 (net charge: $-5e$) changed $\psi(\pm4)$ from −0.690 V to −0.676 V [Figs. 1 and 2(a); systems 1 and 3]. That is, all things being equal, the introduction of PIP2 depolarized the membrane and changed the V_m from ∼−29 mV to ∼−15 mV (compare systems 1 and 3 in Fig. 2). The same conclusion could be reached when the simulations were repeated by replacing the sodium ion with the potassium ion, where the V_m has changed from ∼0 mV in the PC-PC/PS/K system to ∼+20 mV in the PC-PS/PS/PIP2/K system (compare systems 2 and 4 in Fig. 2). This shows that PIP2 counteracts the polarizing effect POPS, suggesting that the effect of anionic lipids on V_m is not limited to their charge content. To check this further, we ran two additional simulations (in the presence of Na^+) in which PIP2 was protonated at either the 4- or 5-position, thus reducing the effective charge by $-1e$ per PIP2 molecule. We obtained almost identical results for the protonated and regular PIP2 systems

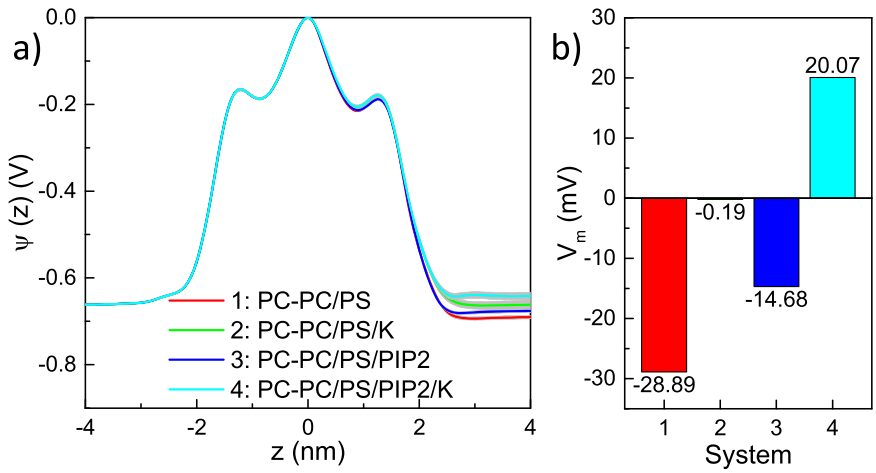

FIG. 2. Effects of membrane asymmetry on electrostatic potential profiles, $\psi(z)$, and transmembrane potential difference, V_m. (a) Static potential profile $\psi(z)$ across model membranes with asymmetric lipid composition and ion distribution. (b) The transmembrane potential difference V_m in the four asymmetric membrane systems.

(Fig. S2). Previous work has found that an asymmetric distribution of charge-neutral cholesterol molecules in the two membrane leaflets changes the V_m.[16] Together, these observations indicate that the effect of PS and PIP2 on the V_m is probably a consequence of structure, dynamics, and specific interactions with ions rather than charge alone.

Asymmetric ion type distribution differently affects V_m

In addition to lipid compositional asymmetry, the plasma membrane is also characterized by an asymmetric distribution of different ions. As shown Fig. 2, replacing Na^+ by K^+ in the PC/PS and PC/PS/PIP2 bilayers increased the electrostatic potential $\psi(\pm 4)$ from −0.690 V to −0.663 V and from −0.676 V to −0.641 V, respectively [Figs. 1 and 2(a)]. Correspondingly, the effective V_m values for systems PC-PC/PS, PC-PC/PS/K, PC-PC/PS/PIP2, and PC-PC/PS/PIP2/K are ~ −29 mV, 0 mV, ~−15 mV, and 20 mV [Fig. 2(b)]. This shows that relative to Na^+, K^+ depolarized the PC-PC/PS system by nearly 30 mV and the PC-PC/PS/PIP2 system by 45 mV. This is a dramatic effect, but qualitatively consistent with the effect of K^+, resulting in a drop in the electrostatic potential across a pure dipalmitoylphosphatidylcholine (DPPC) bilayer observed in a previous simulation by Lee and co-workers.[27] A similar observation has been made in a previous simulation of a POPC/1-palmitoyl-2-oleoyl-sn-*glycero*-3-phosphoethanolamine (POPE) bilayer.[28] In this study, K^+ was found to neutralize the intrinsic transmembrane potential in an asymmetric POPC (outer)/POPE (inner) bilayer. This is also consistent with more complicated bilayer systems consisting of PC, sphingomyelin, PE, PS, and cholesterol molecules.[16] From Table 1 of Ref. 16, we clearly found that the amplitude of the reduction in membrane boundary potential in the presence of Na^+ ions is generally larger than that of K^+ ions, which is consistent with the depolarization effect of K^+ ions discussed in the current work. Together, these observations suggest that the electrostatic interaction of sodium and potassium ions with lipids, and hence their local distribution in and near the bilayer, is completely different, despite their identical charge. We conclude that the interplay among the various ion–lipid interactions—rather than just the charge—is critical for the magnitude and direction of the transmembrane potential.

In addition to Na^+ and K^+ ions, previous studies have shown that Ca^{2+} affects the head-group conformation[29] as well as the dynamics and clustering[30] of PIP2, suggesting a potential role of Ca^{2+} in regulating V_m. However, in simulations with the CHARMM force field, Ca^{2+} tends to interact with lipids unphysically strongly,[31] and while efforts have been made to adjust the interactions of Ca^{2+} with PC and PS lipids via the non-bonded fix (NBFIX) correction in the CHARMM force field,[32,33] no similar study has been carried out for PIP2. Therefore, Ca^{2+} has not been included in the current study, but it should be an interesting topic for future studies.

Differential interactions of Na^+ and K^+ with lipids underlie their differential effect on V_m

To examine how and the extent to which differential cation–lipid interactions modulate the magnitude and direction of V_m, we quantified the time- and ensemble-averaged contact probability Na^+ and K^+ with each atom of each lipid type (Fig. 3). As expected, electrostatic interactions dominate the ion–lipid contacts so that the PIP2 head group (net charge: $-5e$) exhibits the largest contact probability. In addition, compared to the POPC pure bilayer, the presence of the anionic lipids strengthened the adsorption of the two cations onto the membrane.[34] From the plots of the radial distribution function of each ion around the lipid oxygen atoms (Fig. S4), one can clearly see that, overall, K^+'s interactions with the membrane lipids are much weaker than Na^+, which is consistent with the previous work by Lee *et al.*[27] However, the differences in interactions are lipid type-specific so that, relative to Na^+, the interaction of K^+ with PIP2 is greatly reduced, those with POPC are somewhat weakened, whereas the K^+–POPS interaction is even slightly enhanced. The dominant interactions of Na^+ are with PIP2 lipids, followed by a weak preference for POPC and a surprisingly negligible preference for POPS. K^+ maintains the same order of lipid preference (PIP2 > POPC > POPS), but its ability to discriminate among the three lipid types is much less pronounced compared to Na^+. These differential affinities of Na^+ and K^+ for PC, PS, and PIP2 lipids, coupled with the larger aggregate number of Na^+ sequestered by PIP2, likely

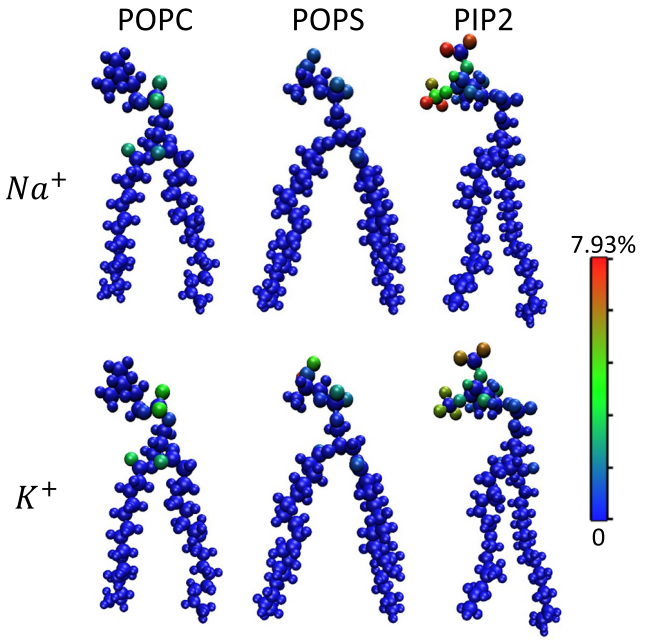

FIG. 3. Contact probability (cutoff = 0.3 nm) between ions (Na^+ or K^+) and lipids for the systems PC/PS/PIP2 and PC/PS/PIP2/K. Lipid atoms were colored blue through red based on their contact probability with the ions (the contact portability with all atoms of all lipids is 100%). The same overall trend is obtained using larger cutoff values for contact definition (Fig. S3).

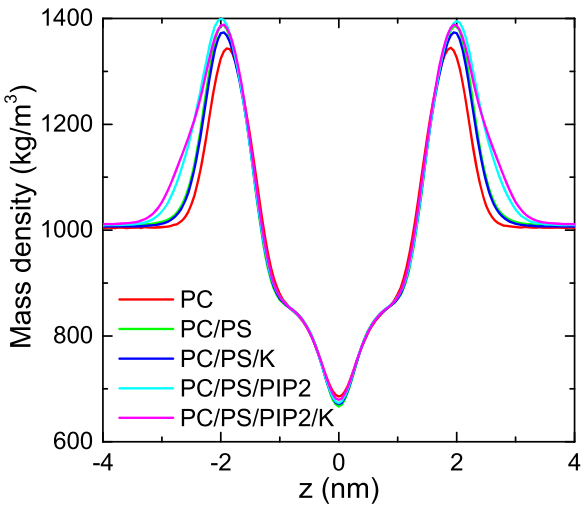

FIG. 4. Mass density distribution profile of the model membrane systems studied in this work.

explain the depolarizing effect of K^+ relative to Na^+ (compare system PC-PC/PS with PC-PC/PS/K and system PC-PC/PS/PIP2 with PC-PC/PS/PIP2/K; Fig. 2). Taken together, the differential interactions of the two cations with the anionic moieties of the three lipid types explain their dramatically different effects on the direction and magnitude of the effective transmembrane potential of the asymmetric systems studied in this work.

Structural details of the membrane systems simulated in this work

Changes in membrane composition could alter lipid–ion interactions, which, in turn, can affect the transmembrane potential. To quantitatively investigate this issue, we calculated the mass density distribution and the acyl chain order of each simulated system. As shown in Fig. 4, the addition of POPS or POPS/PIP2 in the PC bilayer affected the mass density distribution along the membrane normal. For example, relative to the pure PC system, the membrane thickness (peak-to-peak distance in Fig. 4) increased by approximately the same magnitude in both PC/PS and PC/PS/PIP2. Furthermore, Na^+ increased the thickness of the PC/PS/PIP2 bilayer slightly more than K^+ (compare cyan and magenta in Fig. 4). Similarly, the width and height of the mass density distributions indicate differential adsorption of the ions across the head-group region. These effects are directly correlated with the differential impact of the cations on the V_m (Fig. 2). Note that the difference in peak height and width of the distributions among PC, PC/PS, and PC/PS/PIP2 bilayers in the presence of Na^+ (i.e., red, green, and cyan in Fig. 4) is largely due to the larger size of the head group in PS and PIP2 relative to PC [see Fig. 6(a)]. In addition, the local area per lipid can directly affect the lipid–ion interactions.[35] Using APL@Voro[36] for the quantification of the local areas per lipid and focusing on the dominant POPC lipids (70%), we found that the presence of POPS or PIP2 slightly decreases and K^+ slightly increases the average area per lipid (Fig. S5). This is consistent with our inferences from the mass density profiles described above (e.g., PS and PIP2 slightly increased the bilayer thickness, which is consistent with a decrease in area per lipid). Together, these results highlight how membrane composition alters lipid–ion interactions and thereby the V_m.

We then calculated the hydrogen nuclear magnetic resonance (NMR) order parameter for each chain (sn-1 and sn-2) of each lipid type in the five symmetric membrane systems simulated in this work (Table I). Figure 5 (top) shows that the presence of 30% POPS made both chains of the POPC lipids more ordered [compare system PC (red) and PC/PS (green)]. This, however, could also be due to the presence of more Na^+ ions in the PC/PS bilayer. When one-third of the PS lipids in the PC/PS bilayer is replaced by PIP2, no significant changes occurred to the POPC lipid chain order (Fig. 5, top), although the sn-1 order parameter of the PS lipids is reduced slightly (Fig. 5, middle). The latter is likely due to the even larger number of Na^+ ions in the PC/PS/PIP2 bilayer (see Table I). The role of the cations on the lipid chain order is further demonstrated by the fact that the two cations have different ordering effects: compared to Na^+, K^+ rendered both the POPC and POPS lipid chains slightly disordered, despite the identical number and valence of the two ions in the system (green and blue, cyan and magenta in Fig. 5). This may be partly explained by the slightly higher affinity of K^+ for the PS lipids (Fig. 3 and Fig. S4). Each of these observations is directly concordant with the effect of the cations on the V_m (Fig. 2). We conclude that lipid composition and especially the number and type of cations affect lipid packing and thus the charge density distribution along

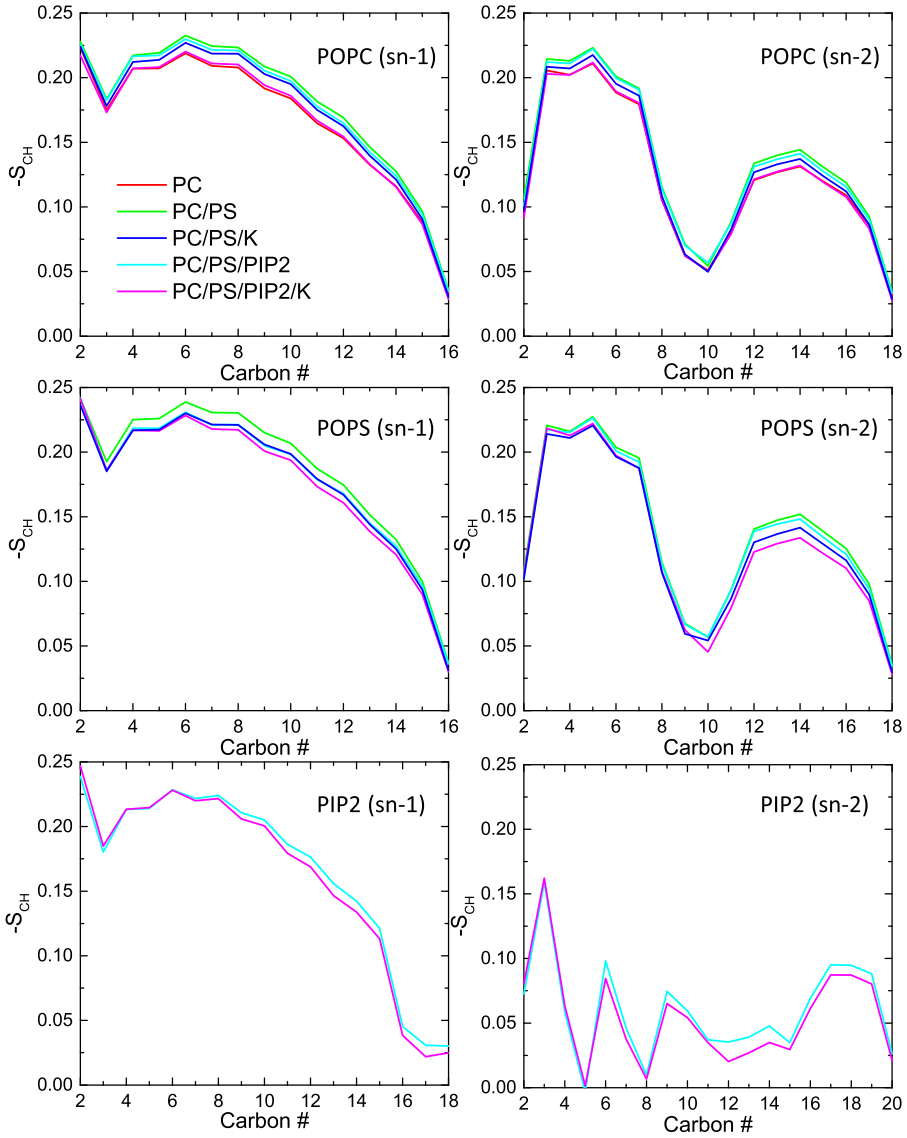

FIG. 5. Lipid chain order parameter of the five simulated symmetric membranes in this work.

the membrane normal, which inevitably modulates the electrostatic potential of the model membranes and thereby the transmembrane potential V_m.

Impact of cation–lipid interactions on lipid head-group orientation

As mentioned above, K^+ ions have a notable effect on the lipid chain order. To further examine the effect of these ions on the membrane structure, we characterized the orientation of lipid head groups in each of the three-component bilayer systems PC/PS/PIP2 and PC/PS/PIP2/K [Fig. 6(b)]. We defined the lipid head-group orientation by the tilt angle from the membrane normal of a vector along the P and N atoms (for PC and PS) and across the six-membered rings (for PIP2), as shown in Fig. 6(a). A smaller tilt angle indicates a better alignment of the lipid head group along the membrane normal, which we refer to as "ordered lipid head orientation." Conversely, when the tilt angle is larger, the head group is considered to be orientationally "disordered." We found that when compared to Na^+, K^+ induced a slight disorder to the POPC lipid head groups and order to the POPS lipid head groups and a more dramatic orientational order to the PIP2 lipid head groups [Fig. 6(c)]. It is intuitive to expect that a decrease in head group orientational disorder is indicative of an increase in area per lipid or a decrease in membrane thickness. This is indeed the case for POPC, where we showed that K^+ slightly increased the area per lipid (Fig S5) and decreased thickness (Fig. 4) relative to Na^+. However, we found no significant differences when we compared the average height of each lipid type in the PC/PS/PIP2 and PC/PS/PIP2/K systems [Fig. 6(d)] (the lipid height averaged over all lipids can be regarded as a

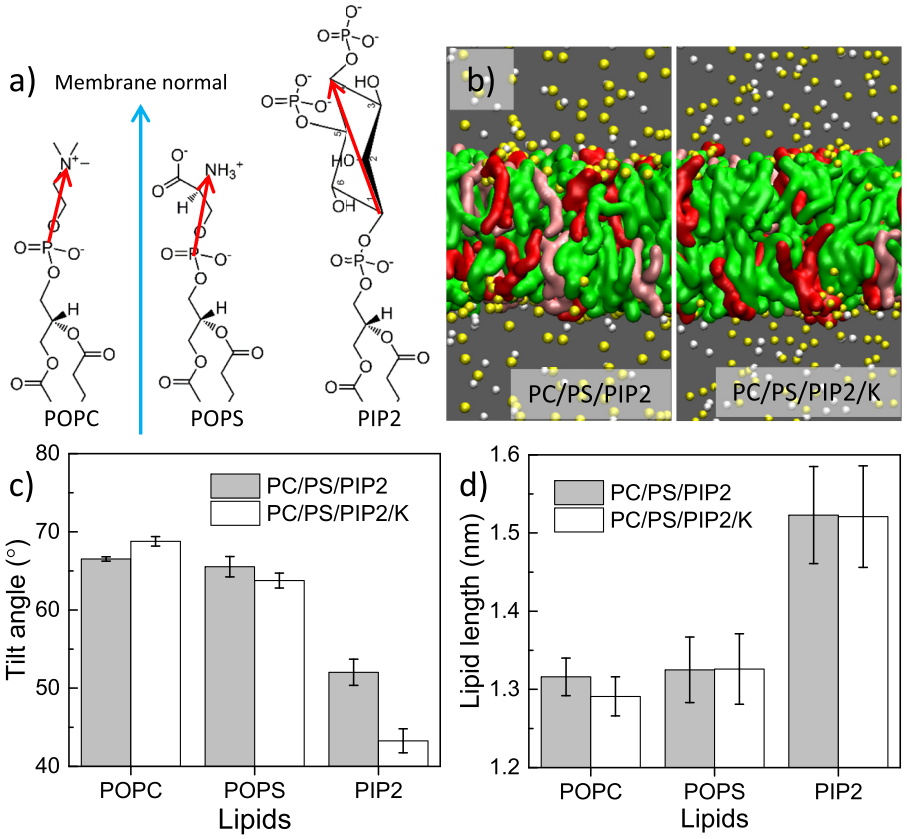

FIG. 6. Effects of Na^+ and K^+ on lipid head-group orientation. (a) Schematics of the vectors used for calculating head-group tilt angles. (b) Snapshots of two systems we have simulated in the presence of Na^+ or K^+, with POPC in green, POPS in pink, PIP2 in red, Na^+ and K^+ in yellow, and Cl^- in white. Water molecules are omitted for clarity. (c) Average tilt angles of the three lipids in the presence of different cations. (d) Average lipid height measured by the distance between the glycerol-phosphate phosphorus atom and the terminal carbon atom of the saturated lipid chains. Errors represent the standard deviation of the average over the last three 300 ns trajectories.

measure of the monolayer thickness). This suggests that the small differences in area per lipid and bilayer thickness between the two systems may be related to the differential domain registration. Combining this with the dramatically different V_m values, we calculated using PC/PS/PIP2 and PC/PS/PIP2/K as models for the inner leaflet an asymmetric membrane (Fig. 2), and it is tempting to speculate a potential correlation between transmembrane potential and membrane asymmetry. Besides, the asymmetric distribution of cholesterol molecules was found to be important in regulating the transmembrane potential (see Table 1 of Ref. 16). Such correlation might be further extended to the local transmembrane potential and the membrane domain (anti)registration,[37–39] where liquid-ordered and liquid-disordered membrane domains have dramatically different ratios of cholesterol, saturated and unsaturated lipids.

In addition to being correlated with the trend of the V_m [Fig. 2(b)], the effect of the cations on head-group orientation is broadly affected by the strength of their interaction with anionic moieties in the different lipids (see Fig. 3), which is consistent with deuterium nuclear magnetic resonance (NMR) studies on effects of various cations on the membrane lipid head groups.[40,41] In these studies, the authors found that compared to K^+ ions, Na^+ ions buried deeper into the membrane and thus had stronger interactions by contacting choline head groups of POPC lipids and serine head groups of POPS lipids, which is partly correlated with the amplitude of ion-induced head group perturbations. In our work, when ranked by the contact probability with the ester phosphate of POPC, the carboxyl group of POPS, and the sugar phosphate of PIP2, we obtain $Na^+ > K^+$, $Na^+ < K^+$, and $Na^+ > K^+$, respectively. When ranked by lipid head-group orientational *order*, the trend is $Na^+ > K^+$, $Na^+ < K^+$, and $Na^+ < K^+$, respectively [Fig. 6(c)]. The imperfect correlation suggests that the differential effect of the ions on lipid head orientation may also be affected by non-specific ion–lipid interactions. This can be captured qualitatively by examining the extent to which the cations are adsorbed on the membrane surface. As shown Fig. 6(b), there are differences in the generalized adsorption of the different ions on the membrane. While both Na^+ and K^+ ions tend to dynamically exchange with ions in the bulk water, on average somewhat more K^+ ions exist in the bulk water, consistent the weaker interactions of K^+ with the lipid membrane discussed above.[27] Taken together and assuming negligible force field artifacts, these results suggest that induction of head-group orientational disorder in the zwitterionic POPC and order in the anionic POPS and PIP2 lipids by a cation such as K^+ depolarizes an asymmetric PC-PC/PS/PIP2 bilayer.

Overall, our simulations suggest that, at least for POPS and PIP2 lipids, the impact of lipid anionic charge on the transmembrane potential difference could be dramatically different and depends not only on charge content but also on structure and dynamics. Different lipid species and ion types can bring about different ion–lipid and lipid–lipid interactions that jointly regulate

the membrane equilibrium structure and charge distribution along the membrane normal. Hence, steady state or transient asymmetric alterations in either lipid composition or ion distribution in the intracellular and extracellular space of the cell may cause major changes in the transmembrane potential difference, V_m.

CONCLUSION

In this work, symmetric model membrane systems were used in all-atom MD simulations to evaluate the electrostatic potential profiles of physiologically relevant asymmetric membranes. Averaging of the two halves of symmetric membrane systems can ensure the symmetric charge density distribution around the membrane center, which yields a reliable $\psi(z)$ profile and thus eliminates a *non-zero* V_m in multi-component symmetric model membranes. We have shown that one could obtain a recombinant $\psi(z)$ profile for an asymmetric membrane by combining two symmetrized $\psi(z)$ profiles obtained from two independent MD simulations, one modeling the inner leaflet and another modeling the outer leaflet of the plasma membrane. In the current work, a pure POPC bilayer in a 150 mM NaCl solution was used as a model for the outer half of the plasma membrane. The inner leaflet was modeled by a two-component POPC/POPS and a three-component POPC/POPS/PIP2 bilayer in the presence of neutralizing Na^+ ions. The POPC/POPS and POPC/POPS/PIP2 bilayers were also simulated after replacing Na^+ with K^+ ions. Comparison of the effective transmembrane potential difference V_m obtained from combining the $\psi(z)$ profiles of the POPC bilayer with each of the inner leaflet model membranes indicates that POPS in the inner leaflet polarizes the membrane ($\Delta V_m < 0$), whereas replacing a third of the PS lipids by PIP2 partially counteracts this effect. Furthermore, replacing intracellular Na^+ by K^+ depolarizes the membrane ($\Delta V_m > 0$). We have shown that these differential effects are a result of differential cation–lipid interactions and are correlated with changes in lipid structure and head-group orientation.

SUPPLEMENTARY MATERIAL

See the supplementary material for five additional figures.

ACKNOWLEDGMENTS

This work was supported by the National Natural Science Foundation of China (Grant No. 21903002), the Fundamental Research Funds for the Central Universities (Grant No. YWF-20-BJ-J-632), the Open Fund of State Key Laboratory of Membrane Biology (Grant No. 2020KF09; X.L.), and the NIH (Grant No. R01GM124233; A.A.G.). We are grateful to the Texas Advanced Computing Center (TACC), the Extreme Science and Engineering Discovery Environment (XSEDE), and the Supercomputing Center of Beihang University for generous computing resources. We thank the anonymous reviewers for insightful comments on our manuscript. X.L. also thanks his quiet and smart newborn baby for creating sufficient time for him to revise this manuscript.

The authors declare no competing financial interest.

DATA AVAILABILITY

The data that support the findings of this study are available from the corresponding authors upon the request. In addition, MD trajectories with the reduced frame-saving frequency can be directly accessed from the open-access repository zenodo.org (https://doi.org/10.5281/zenodo.3968113).

REFERENCES

[1] B. Alberts, A. Johnson, J. Lewis, D. Morgan, M. Raff, K. Roberts, and P. Walter, *Molecular Biology of the Cell*, 6th ed. (Garland Press, New York, 2014).
[2] Y. Shu, A. Hasenstaub, A. Duque, Y. Yu, and D. A. McCormick, "Modulation of intracortical synaptic potentials by presynaptic somatic membrane potential," Nature **441**, 761–765 (2006).
[3] X. Gao, S. Hong, Z. Liu, T. Yue, J. Dobnikar, and X. Zhang, "Membrane potential drives direct translocation of cell-penetrating peptides," Nanoscale **11**, 1949–1958 (2019).
[4] G. Thrivikraman, S. K. Boda, and B. Basu, "Unraveling the mechanistic effects of electric field stimulation towards directing stem cell fate and function: A tissue engineering perspective," Biomaterials **150**, 60–86 (2017).
[5] M. Yang and W. J. Brackenbury, "Membrane potential and cancer progression," Front. Physiol. **4**, 185 (2013).
[6] Y. Zhou, C.-O. Wong, K.-j. Cho, D. van der Hoeven, H. Liang, D. P. Thakur, J. Luo, M. Babic, K. E. Zinsmaier, M. X. Zhu, H. Hu, K. Venkatachalam, and J. F. Hancock, "Membrane potential modulates plasma membrane phospholipid dynamics and K-Ras signaling," Science **349**, 873–876 (2015).
[7] G. Van Meer, D. R. Voelker, and G. W. Feigenson, "Membrane lipids: Where they are and how they behave," Nat. Rev. Mol. Cell Biol. **9**, 112 (2008).
[8] K. R. Levental, J. H. Lorent, X. Lin, A. D. Skinkle, M. A. Surma, E. A. Stockenbojer, A. A. Gorfe, and I. Levental, "Polyunsaturated lipids regulate membrane domain stability by tuning membrane order," Biophys. J. **110**, 1800–1810 (2016).
[9] L. Delemotte, F. Dehez, W. Treptow, and M. Tarek, "Modeling membranes under a transmembrane potential," J. Phys. Chem. B **112**, 5547–5550 (2008).
[10] J. Melcr, D. Bonhenry, Š. Timr, and P. Jungwirth, "Transmembrane potential modeling: Comparison between methods of constant electric field and ion imbalance," J. Chem. Theory Comput. **12**, 2418–2425 (2016).
[11] N. Basdevant, D. Dessaux, and R. Ramirez, "Ionic transport through a protein nanopore: A coarse-grained molecular dynamics study," Sci. Rep. **9**, 15740 (2019).
[12] R. A. Böckmann, A. Hac, T. Heimburg, and H. Grubmüller, "Effect of sodium chloride on a lipid bilayer," Biophys. J. **85**, 1647–1655 (2003).
[13] X. Lin, V. Nair, Y. Zhou, and A. A. Gorfe, "Membrane potential and dynamics in a ternary lipid mixture: Insights from molecular dynamics simulations," Phys. Chem. Chem. Phys. **20**, 15841–15851 (2018).
[14] H. Li, J. Chowdhary, L. Huang, X. He, A. D. MacKerell, and B. Roux, "Drude polarizable force field for molecular dynamics simulations of saturated and unsaturated zwitterionic lipids," J. Chem. Theory Comput. **13**, 4535–4552 (2017).
[15] J. Huang, S. Rauscher, G. Nawrocki, T. Ran, M. Feig, B. L. de Groot, H. Grubmüller, and A. D. MacKerell, "CHARMM36m: An improved force field for folded and intrinsically disordered proteins," Nat. Methods **14**, 71–73 (2017).
[16] S. G. Falkovich, H. Martinez-Seara, A. M. Nesterenko, I. Vattulainen, and A. A. Gurtovenko, "What can we learn about cholesterol's transmembrane distribution based on cholesterol-induced changes in membrane dipole potential?," J. Phys. Chem. Lett. **7**, 4585–4590 (2016).
[17] S. Jo, T. Kim, V. G. Iyer, and W. Im, "CHARMM-GUI: A web-based graphical user interface for CHARMM," J. Comput. Chem. **29**, 1859–1865 (2008).
[18] J. Lee, X. Cheng, J. M. Swails, M. S. Yeom, P. K. Eastman, J. A. Lemkul, S. Wei, J. Buckner, J. C. Jeong, Y. Qi, S. Jo, V. S. Pande, D. A. Case, C. L. Brooks, A. D. MacKerell, J. B. Klauda, and W. Im, "CHARMM-GUI input generator for NAMD, GROMACS, AMBER, OpenMM, and CHARMM/OpenMM simulations using

the CHARMM36 additive force field," J. Chem. Theory Comput. **12**, 405–413 (2016).
[19]S. Nosé, "A molecular dynamics method for simulations in the canonical ensemble," Mol. Phys. **52**, 255–268 (1984).
[20]W. G. Hoover, "Canonical dynamics: Equilibrium phase-space distributions," Phys. Rev. A **31**, 1695–1697 (1985).
[21]M. Parrinello and A. Rahman, "Polymorphic transitions in single crystals: A new molecular dynamics method," J. Appl. Phys. **52**, 7182–7190 (1981).
[22]B. Hess, H. Bekker, H. J. C. Berendsen, and J. G. E. M. Fraaije, "LINCS: A linear constraint solver for molecular simulations," J. Comput. Chem. **18**, 1463–1472 (1997).
[23]U. Essmann, L. Perera, M. L. Berkowitz, T. Darden, H. Lee, and L. G. Pedersen, "A smooth particle mesh Ewald method," J. Chem. Phys. **103**, 8577–8593 (1995).
[24]M. J. Abraham, T. Murtola, R. Schulz, S. Páll, J. C. Smith, B. Hess, and E. Lindahl, "GROMACS: High performance molecular simulations through multi-level parallelism from laptops to supercomputers," SoftwareX **1-2**, 19–25 (2015).
[25]W. Humphrey, A. Dalke, and K. Schulten, "VMD: Visual molecular dynamics," J. Mol. Graphics **14**, 33–38 (1996).
[26]A. A. Gurtovenko and I. Vattulainen, "Membrane potential and electrostatics of phospholipid bilayers with asymmetric transmembrane distribution of anionic lipids," J. Phys. Chem. B **112**, 4629–4634 (2008).
[27]S.-J. Lee, Y. Song, and N. A. Baker, "Molecular dynamics simulations of asymmetric NaCl and KCl solutions separated by phosphatidylcholine bilayers: Potential drops and structural changes induced by strong Na^+-lipid interactions and finite size effects," Biophys. J. **94**, 3565–3576 (2008).
[28]A. A. Gurtovenko and I. Vattulainen, "Intrinsic potential of cell membranes: Opposite effects of lipid transmembrane asymmetry and asymmetric salt ion distribution," J. Phys. Chem. B **113**, 7194–7198 (2009).
[29]E. Bilkova, R. Pleskot, S. Rissanen, S. Sun, A. Czogalla, L. Cwiklik, T. Róg, I. Vattulainen, P. S. Cremer, P. Jungwirth, and Ü. Coskun, "Calcium directly regulates phosphatidylinositol 4, 5-bisphosphate headgroup conformation and recognition," J. Am. Chem. Soc. **139**, 4019–4024 (2017).
[30]Y. Wen, V. M. Vogt, and G. W. Feigenson, "Multivalent cation-bridged PI(4,5)P2 clusters form at very low concentrations," Biophys. J. **114**, 2630–2639 (2018).
[31]A. Catte, M. Girych, M. Javanainen, C. Loison, J. Melcr, M. S. Miettinen, L. Monticelli, J. Määttä, V. S. Oganesyan, O. H. S. Ollila, J. Tynkkynen, and S. Vilov, "Molecular electrometer and binding of cations to phospholipid bilayers," Phys. Chem. Chem. Phys. **18**, 32560–32569 (2016).
[32]K. Han, R. M. Venable, A.-M. Bryant, C. J. Legacy, R. Shen, H. Li, B. Roux, A. Gericke, and R. W. Pastor, "Graph–theoretic analysis of monomethyl phosphate clustering in ionic solutions," J. Phys. Chem. B **122**, 1484–1494 (2018).
[33]S. Kim, D. S. Patel, S. Park, J. Slusky, J. B. Klauda, G. Widmalm, and W. Im, "Bilayer properties of lipid A from various gram-negative bacteria," Biophys. J. **111**, 1750–1760 (2016).
[34]P. Jurkiewicz, L. Cwiklik, A. Vojtíšková, P. Jungwirth, and M. Hof, "Structure, dynamics, and hydration of POPC/POPS bilayers suspended in NaCl, KCl, and CsCl solutions," Biochim. Biophys. Acta, Biomembr. **1818**, 609–616 (2012).
[35]M. Javanainen, A. Melcrová, A. Magarkar, P. Jurkiewicz, M. Hof, P. Jungwirth, and H. Martinez-Seara, "Two cations, two mechanisms: Interactions of sodium and calcium with zwitterionic lipid membranes," Chem. Commun. **53**, 5380–5383 (2017).
[36]G. Lukat, J. Krüger, and B. Sommer, "APL@Voro: A voronoi-based membrane analysis tool for GROMACS trajectories," J. Chem. Inf. Model. **53**, 2908–2925 (2013).
[37]S. Zhang and X. Lin, "Lipid acyl chain *cis* double bond position modulates membrane domain registration/anti-registration," J. Am. Chem. Soc. **141**, 15884–15890 (2019).
[38]J. D. Perlmutter and J. N. Sachs, "Interleaflet interaction and asymmetry in phase separated lipid bilayers: Molecular dynamics simulations," J. Am. Chem. Soc. **133**, 6563–6577 (2011).
[39]J. D. Nickels, J. C. Smith, and X. Cheng, "Lateral organization, bilayer asymmetry, and inter-leaflet coupling of biological membranes," Chem. Phys. Lipids **192**, 87–99 (2015).
[40]M. Roux and M. Bloom, "Calcium, magnesium, lithium, sodium, and potassium distributions in the headgroup region of binary membranes of phosphatidylcholine and phosphatidylserine as seen by deuterium NMR," Biochemistry **29**, 7077–7089 (1990).
[41]M. Roux and J.-M. Neumann, "Deuterium NMR study of head-group deuterated phosphatidylserine in pure and binary phospholipid bilayers: Interactions with monovalent cations Na^+ and Li^+," FEBS Lett. **199**, 33–38 (1986).